

Absolute line strengths for carbon and sulfur*

Myron H. Miller, Thomas D. Wilkerson, and Randy A. Roig†

Institute for Fluid Dynamics and Applied Mathematics, University of Maryland, College Park, Maryland 20742

Roger D. Bengtson

Department of Physics, University of Texas at Austin, Austin, Texas 78712

(Received 21 November 1973)

Absolute transition probabilities for 124 C I, S I, and S II lines in the range 3600–7400 Å are measured with a spectroscopic shock tube. Relative strengths of two C II lines are also determined. Mixtures of neon and ten different compounds of carbon and sulfur are heated to temperatures 8200–13000°K at pressures $(4.8\text{--}27.0) \times 10^6$ dyn cm⁻². Thermodynamic and photometric variables are measured redundantly. Absolute A values are determined in emission by two or more independent methods which in combination have much less than the traditional sensitivity to systematic errors in source temperature. Estimated accuracies for the more prominent visible lines are 13–30%. Results are compared with theoretical predictions, other experiments, and with quantum-mechanical sum rules.

I. INTRODUCTION

Strengths of visible carbon and sulfur lines have been measured using a variety of spectroscopic light sources, but results to date have tended to disagree by approximately a factor of 2.^{1–8} The present work substantially reduces uncertainties in the line strengths of these theoretically and astrophysically important elements.^{9–12} Our spectroscopic techniques are less error prone than those traditionally employed for transitions between highly excited states. All essential experimental variables are measured redundantly. Proper selection of operating conditions brings the more prominent C I, S I, and S II lines to comparable brightness at electron densities small enough that Stark broadening does not blend the three spectra. The shock-heating of CH₃SH fixes the carbon-to-sulfur abundance ratio, allowing carbon and sulfur A values to be related in a direct and simple way.

II. EXPERIMENTAL

To minimize the likelihood of the systematic errors often associated with A values measured in emission,^{12,13} we observed the following precautions:

(i) Absolute line strengths were obtained by techniques selected for their small sensitivity to possible bias in temperature data and photometric calibrations.

(ii) Two or more independent methods were used to measure thermodynamic variables and to calibrate detectors for absolute sensitivity and spectral response.

(iii) Conditions in the light source (temperature, density, composition) and instrumental parameters (spectroscopic recording materials, slit widths, sampling times) were deliberately varied in a search for possible error trends in the atomic data.

Plasmas behind reflected shock waves were homogeneous and quiescent for periods of 30–150 μsec. Electron densities were generally $(2\text{--}16) \times 10^{16}$ cm⁻³, a range which maintains local thermodynamic equilibrium (LTE) for temperatures of $(8200\text{--}13000)^\circ\text{K}$.¹⁴ Plasma durations were too short to permit significant demixing of heavier and lighter constituents. Therefore, the initial chemical composition and two plasma-state variables uniquely specify the populations of all atomic and ionic levels in the light source.

Computed emitter densities can be combined with photometric data in two ways to determine an absolute transition probability A_{mn} . By recording the absolute integrated intensity I_{mn} of an isolated optically thin line of wavelength λ_{mn} , we have

$$A_{mn}^{em} = \frac{I_{mn} 4\pi\lambda_{mn}}{hcl N_m(p, T)}, \quad (1)$$

where l is the thickness of the light source and $N_m(p, T)$ is the excited-state density. If the plasma emits some other line λ_{pq} , whose transition probability A_{pq} is well known, then a measurement of the intensity ratio I_{mn}/I_{pq} will also yield a value for A_{mn} :

$$A_{mn}^{r, pq} = A_{pq} \frac{\lambda_{mn} I_{mn} N_p(p, T)}{\lambda_{pq} I_{pq} N_m(p, T)}. \quad (2)$$

For example, shock heating a gas containing

TABLE I. Techniques used to measure absolute A values.

Spectrum method	A value or intensity standard
$A_C^{\text{em}} = \frac{4\pi I_C \lambda_C}{h c I N_C}$ $A_C^{\text{r,H}} = A \frac{I_C \lambda_C N_H}{I_H \lambda_H N_C}$	Carbon arc anode (Ref. 15) and blackbody shock-tube plasmas (Ref. 16). Usually H_β , but occasionally H_γ .
$A_S^{\text{em}} = \frac{4\pi I_S \lambda_S}{h c I N_S}$ $A_S^{\text{r,H}} = \frac{I_S \lambda_S N_H}{I_H \lambda_H N_S}$	Carbon arc anode (Ref. 15) and blackbody shock-tube plasmas (Ref. 16). H_β or H_γ , depending upon plasma brightness.
$A_S^{\text{r,C}} = \frac{I_S \lambda_S N_C}{I_C \lambda_C N_S}$	CI ($\lambda = 5052$) ^a
$A_{SII}^{\text{r,H}} = \frac{I_{SII} \lambda_{SII} N_H}{I_H \lambda_H N_{SII}}$ $A_{SII}^{\text{r,Ne}} = \frac{I_{SII} \lambda_{SII} N_{Ne}}{I_{Ne} \lambda_{Ne} N_{SII}}$	H_β Normally Ne I ($\lambda = 5852 \text{ \AA}$); alternatively, Ne I ($\lambda = 5881 \text{ \AA}$)

^aThis line is employed as a "standard" only for purposes of directly relating absolute A values of neutral carbon and sulfur.

methyl mercaptan (CH_3SH) produces a plasma whose constituents are stoichiometrically related. Lines such as CI ($\lambda = 5052 \text{ \AA}$), SI ($\lambda\lambda = 4695 \text{ \AA}$), and SII ($\lambda = 5453 \text{ \AA}$) can be measured relative to H_β , whose A value serves as an internal standard ($A_{p,q}$), given that the corresponding relative abundances are fixed. Hydrogen Balmer lines can be utilized as internal references in six of the ten test gases listed in Table I.

Table I shows the methods used, as a rule simultaneously, to determine absolute CI, SI, and SII line strengths. Intensity standards for the absolute intensity measurements required by Eq. (1) are the anode crater of a regulated carbon arc¹⁵ and the Planck intensity of shock-tube plasmas measured by the line-reversal technique.¹⁶ For the transspecies relative intensity determinations of Eq. (2), the Balmer lines (H_β, H_γ), and the neon red lines [Ne I ($\lambda = 5852 \text{ \AA}$), Ne I ($\lambda = 5881 \text{ \AA}$)] provide reference A values reliable to better than 1% and approximately 10%, respectively.¹²

Densities of excited states for some prominent visible lines are given in Fig. 1 as functions of temperature at a representative operating pressure and composition.¹⁷ Slopes of the curves indicate sensitivity to temperature error for A values measured via Eq. (1): the corresponding sensitivity for data obtained via Eq. (2) is obtained from differences in the slopes.

Figure 2 shows the relative error $A(T)/A(T_0)$ in transition probabilities that would be measured with faulty temperature data. For each of the measurement techniques listed in Table I, the

assumed temperature T is allowed to vary continuously from a true temperature T_0 of 11 000 °K. The mean of the simultaneous A_C^{em} and $A_C^{\text{r,H}}$ determinations shown in Fig. 2(a) cannot underestimate the true A value for CI ($\lambda = 5052 \text{ \AA}$), regardless of the size or direction of temperature error: errors of $\pm 5\%$ in temperature cause an approximate $+5\%$ biasing of results.¹⁸ For the blended multiplet SI ($\lambda\lambda = 4695 \text{ \AA}$), the shot-by-shot

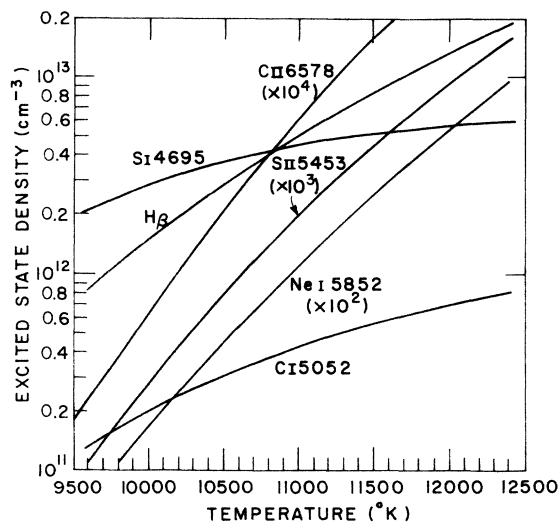


FIG. 1. Temperature dependence of excited-state number densities for lines prominent in shock-tube plasmas. Pressure is $9.0 \times 10^6 \text{ dyn cm}^{-2}$ and test gas (molal) composition is 1.0% CH_3SH + 99.0% neon.

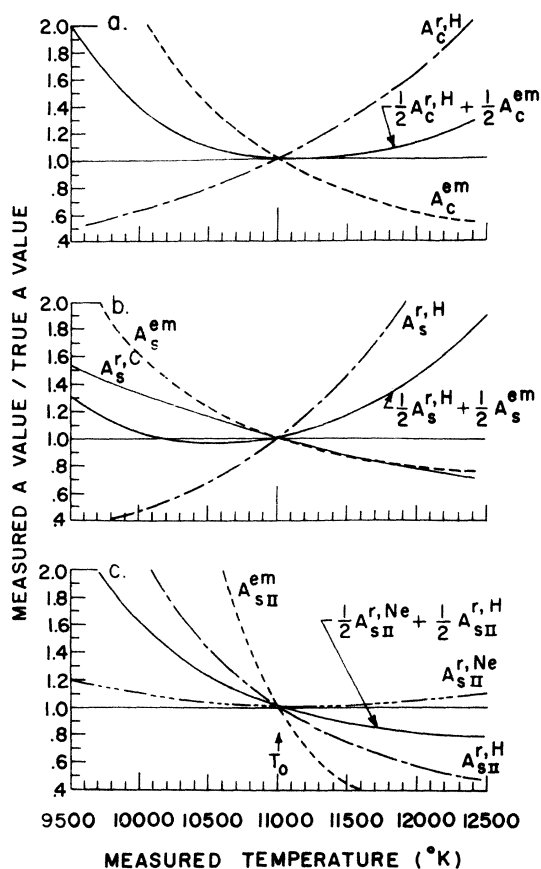


FIG. 2. Relative error in experimental A values determined by various methods, as functions of temperature error $T - T_0$. The true plasma temperature T_0 is 11 000°. Pressure and composition are as in Fig. 1.

mean of A_s^{em} and $A_s^{r,H}$ determinations has a lesser thermal sensitivity than either of these measurements separately, as shown in Fig. 2(b). In contrast to the critical temperature sensitivity of the absolute emission A_{sII}^{em} data for SII ($\lambda = 5453 \text{ \AA}$) determinations via $A_{sII}^{r,H}$ and $A_{sII}^{r,Ne}$ are seen in Fig. 2(c) to be only mildly affected by temperature error.

Test gases, thermodynamic conditions, and spectrographic recording materials used in the experiment are compiled in Table II. Several volatile compounds of carbon and/or sulfur were utilized in order (i) to selectively enhance either H, CI, SI, or SII spectra, (ii) to vary line-to-continuum ratios over factors of 10, and (iii) to test for reaction or absorption of test gas constituents prior to firing the shock tube.

Plasma temperatures and pressures were systematically varied between 8200 and 13 200°K and $(4.8-27.0) \times 10^6 \text{ dyn cm}^{-2}$, respectively. This posed a stringent test for the consistency of redundant state and photometric data, caused line widths due to the Stark effect to vary several fold with respect to instrumental widths, and selectively enhanced the brightness of weaker neutral or ionic lines.

The five emulsions tabulated in the fifth column have distinctly different spectral responses and γ characteristics. Relative line strengths recorded on different materials were routinely checked for any indications of faulty photographic calibration or data-reduction procedures.

Instrumentation for time-resolved spectroscopy¹⁹⁻²² is shown schematically in Fig. 3. Poly-

TABLE II. Summary of experimental conditions.

Runs	Test gas ^a	Temperatures ($10^3 \text{ }^\circ\text{K}$)	Pressures (10^6 dyn cm^{-2})	Photographic emulsions (Kodak)
24	$(\frac{1}{6}-2)\% \text{CH}_4$	9.4-12.9	5.0-19.5	2475
9	$\frac{1}{2}\% \text{CH}_4 + \frac{1}{2}\% \text{CS}_2$	9.8-12.6	6.1-21.9	2475
6	$\frac{1}{2}\% \text{CH}_4 + \frac{1}{2}\% \text{CCl}_4$	10.3-12.2	7.6-18.0	2475, HSIR
7	$(\frac{1}{2}-2\frac{1}{2})\% \text{CH}_3\text{Br}$	9.1-12.0	5.9-18.5	2475, HSIR
12	$(\frac{1}{2}-1\frac{1}{2})\% \text{CH}_3\text{SH}$	9.6-12.7	6.3-23.0	2475, I-N
6	$\frac{1}{2}\% \text{H}_2\text{S} + \frac{1}{2}\% \text{PH}_3$	9.9-12.4	6.0-22.0	2475
6 ^b	1% SO_2	10.8-13.0	3.6-17.2	2475, I-N
3	$\frac{1}{2}\% \text{CH}_3\text{OH}$	11.2-11.8	9.0-12.5	I-F
11	$(\frac{1}{2}-2)\% \text{H}_2\text{S}$	9.6-12.6	4.8-21.8	103-0, I-N, I-F
5	$(\frac{1}{3}-\frac{2}{3})\% \text{Si}[\text{CH}_3]_4$	8.2-11.9	8.6-27.0	2475, I-N

^aThe carrier gas is in all cases Research Grade neon.

^bUnlike other listed experimental runs, these data were used to determine relative rather than absolute A values, particularly for SII that would be masked by Balmer lines in plasmas containing hydrogen.

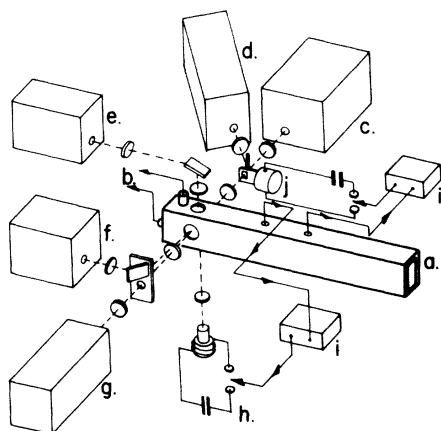


FIG. 3. Diagram of the shock-tube instrumentation: (a) shock-tube test section; windows and associated optics are fused quartz; (b) piezoelectric pressure transducers mounted in the shock tube upper- and end-walls; (c) $\frac{3}{4}$ -m spectrograph; (d) 1-m stigmatic spectrograph; (e) $\frac{1}{2}$ -m monochromator, with photoelectric recording; (h) fast TRW gray-body flashlamp; (f) six-channel $1\frac{1}{2}$ -m photoelectric polychromator, utilizing shaped fibre optics (Ref. 19); (g) twelve-channel, $\frac{1}{2}$ -m polychromator, photoelectrically recording 1.0- \AA wide portions of the H_{β} profile; (i) delay pulsers, triggered by ionization gauges in the shock tube, for firing the flashlamp and the fast shutter, (j) (Ref. 19).

chromators (e), (f), and (g) contain 19 photoelectric channels which are calibrated against the anode of a regulated carbon arc¹⁴ and also by the line-reversal technique.^{16,23,24} Seventeen of these are employed to measure plasma temperature by a number of simultaneous and independent techniques. The excitation temperature²⁵ of H_{β} ($11 < E/kT < 14$), was derived from pressure data and the line's integrated energy. Time-resolved relative-intensity profiles of Balmer lines obtained photographically by spectrometers (c) and (d) were converted to an absolute scale on a shot-by-shot basis by fitting to the signals from 12 absolutely calibrated photoelectric channels in polychromator (f). These photographically recorded H_{β} and/or H_{γ} profiles were also fitted to theoretical Stark shapes²⁶ to give the plasma electron density. Together with measured pressure, this was inverted to find a plasma ionization temperature. Monochromator (e) was centered on H_{α} , which had typical peak optical depths of 0.5–4.0. Viewing the plasma along a path backlit by the pulsed flashlamp (h), these data gave Planck intensity and radiation temperature by the reversal method.^{19,24}

The four measured temperatures usually agreed to within 300 °K. No trends were detected over the experimental range ($\Delta T = 5000$ °K). This sus-

tained agreement between the four types of temperature determinations supports our assumptions regarding plasma homogeneity, extent of laminar boundary layers, and LTE.

Pressures recorded by the two transducers (b) generally agreed to within the 15% precision set by crystal ringing and reading error. The two sensors differed systematically by 6%, which is commensurate with the accuracy of static and dynamic calibrations.

Spectrographs (c) and (d) have first-order resolutions of 2.0 and 0.28 \AA , respectively. Corresponding wavelength coverages are 6000 and 1700 \AA . In early phases of the work, a rotating drum camera^{20,21} provided time-resolved recording. Wavelength resolution and signal levels were subsequently improved by employing a fast mechanical shutter¹⁹ (j) at an intermediate focal position common to spectrographs (c) and (d). As a precaution against bias, the two spectrographs were customarily loaded with plates having different spectral response and γ characteristics. We calibrated all emulsions listed in Table II using a regulated carbon arc and pulsed light sources. Controlled attenuation was provided by (i) a seven-step neutral density filter, (ii) a continuously variable filter, and (iii) photomultipliers situated in the photographic focal plane to monitor light levels as entrance slit-widths were systematically varied. No adjacency or reciprocity effects were found for spectral densities or exposure times of interest.

Computer codes²⁷ for converting digitized photographic densities into intensities utilized absolute photoelectric data and measured temperatures to compensate for radiative trapping. With the exception of CI ($\lambda = 5052$ \AA) the carbon and sulfur line-strength data were obtained from photographically recorded profiles.

Precision in the delineating and integrating of a typical line profile was 15%, with the limiting factors being grain noise, reading error, and uncertainty in discriminating far-wing intensities from the background continuum. The histogram in Fig. 4 illustrates the usual scatter in relative A values due to random errors in the areas of two-line profiles. The distribution appears to be Gaussian, with a 23% standard deviation. Typically, precision was poorer than this for the weak and broadened SI lines, but slightly better for prominent SII lines.

The energy radiated in CI ($\lambda = 5052$ \AA) was simultaneously recorded in two ways—photographically and by a pair of photoelectric channels. Measured Stark widths were used to adjust²¹ for far-wing contributions cut off by the 2.0- \AA photoelectric channel widths. The two sets of

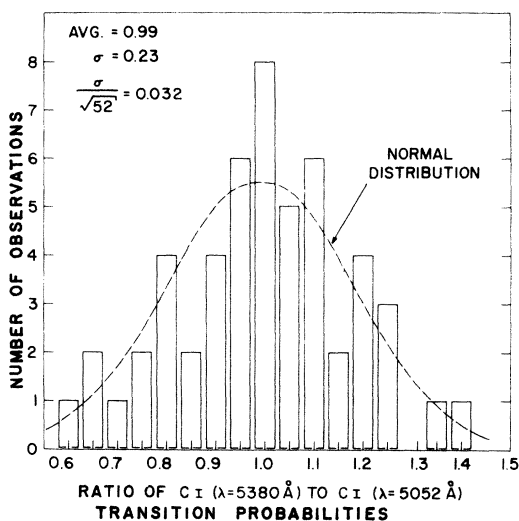


FIG. 4. Histogram of the measured ratio of C I ($\lambda = 5380 \text{ \AA}$) to C I ($\lambda = 5052 \text{ \AA}$) A values, illustrating typical scatter due to relative photographic photometry with fast, grainy emulsions.

integrated C I ($\lambda = 5052 \text{ \AA}$) line intensities agreed on the average to 6%, with approximately 20% scatter.

III. RESULTS AND DISCUSSION

Results of the C I ($\lambda = 5052 \text{ \AA}$) transition-probability measurements by the A_C^{em} , $A_C^{\text{r,H}}$ and $\frac{1}{2}(A_C^{\text{em}} + A_C^{\text{r,H}})$ techniques are compared in Fig. 5. The

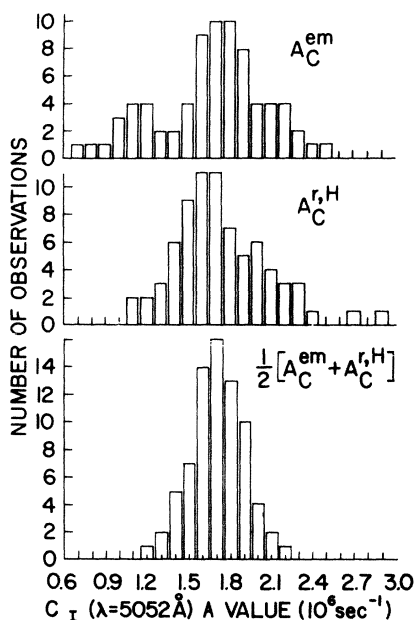


FIG. 5. Histogram of results from various simultaneous measurements of the absolute C I ($\lambda = 5052 \text{ \AA}$) A value.

A_C^{em} and $A_C^{\text{r,H}}$ distributions are approximately twice as wide as the distribution of their shot-by-shot average $\frac{1}{2}(A_C^{\text{em}} + A_C^{\text{r,H}})$. Analysis based on Fig. 2(a) attributes this difference to (2–4)% random error in temperature data, and indicates that the centroid of the $\frac{1}{2}(A_C^{\text{em}} + A_C^{\text{r,H}})$ results has been shifted upwards by approximately 3%. The adopted C I ($\lambda = 5052 \text{ \AA}$) transition probability ($1.60 \times 10^6 \text{ sec}^{-1}$) has been compensated for this systematic effect of random error.^{27a}

No correlation was found between measured carbon A values and experimental temperatures, plasma pressures, and electron density. If laminar boundary layers, whose thickness scale inversely with pressure,²³ were spectroscopically important, or if LTE conditions were not attained, such independence would not be expected. Results obtained using the different test gases and recording materials listed in Table II were indistinguishable from one another.

Neutral carbon A values are presented in Table III. Our uncertainties are expressed as 67% confidence limits, and are based on estimates of possible experimental bias and on statistical analysis of scatter. In the majority of runs where the electron density was greater than $4 \times 10^{16} \text{ cm}^{-3}$, the strength of multiplet 6 was measured because Stark broadening merged the individual lines. Faint lines such as C I ($\lambda = 5817 \text{ \AA}$) did not attain useful brightness under most conditions. The relatively prominent C I ($\lambda = 4932 \text{ \AA}$) line and the blended C I ($\lambda = 5041 \text{ \AA}$) multiplet were particularly diffuse.

Carbon data from the shock tube tend to be factors of 1.2–2.8 smaller than strengths predicted by the central field approximations. It should be noted that the majority of transitions have core-penetrating (s) lower states and thus do not satisfy the reliability criteria^{30,31} for use of the Coulomb approximation.

Foster^{4,5} used a vortex-stabilized arc to make absolute emission (A_C^{em}) determinations. Ratios of vortex-arc A values to the present findings average 0.97 and 0.82 for the earlier⁴ and later⁵ of his investigations.

Wall-stabilized multicomponent arcs were the light sources employed by Beth,¹ Richter,¹ Kuck,¹ and Maecker.¹ It has been suggested^{10,12} that the absolute scales of these (A_C^{em}) results were biased by unrecognized demixing. Considering their generic similarity, it is surprising that the absolute and relative A values obtained in these four investigations are not closer to mutual agreement than are the results from pairs of investigations having less similarity in experimental approach.

To circumvent the difficulties stemming from

TABLE III. Transition probabilities for neutral carbon (10^6 sec^{-1}).

Multiplet ^{28, 29}	$g_i - g_k$	λ (Å)	This work	NBS ¹² (1966)	Henning ² (1965)	Foster ⁵ (1962)	Foster ⁴ (1962)	Doherty ³ (1961)	Beth ¹ (1963)	Richter ² (1958)	Kueck ¹ (1955)	Maecker ¹ (1953)	ca-LS ^{30,31}
(4)	9-15	$\lambda\lambda = 5041$	0.19 ^a	0.39		0.13	0.21			0.30		0.15	1.55
(5)	5-3	4826.7	0.10 ± 40%	0.47		0.34							0.24
	3-3	4817.3	0.06 ± 40%	0.28									0.14
	1-3	4812.8	<0.03	0.10									0.05
(6)	9-9	$\lambda\lambda = 4770$	1.53 ± 15%	1.6	0.80	0.95	1.26	1.8	1.0	1.2	0.44	0.52	1.34
	5-5	4771.7	1.2	1.2									1.01
	3-1	4770.0	1.00 ± 30%	1.5									1.26
	3-3	4766.6	0.48 ± 30%	0.39									0.33
	5-3	4775.9	0.67 ± 30%	0.62									0.52
	3-5	4762.4	0.38	0.38									0.32
	1-3	4762.4	0.50 ± 30%	0.52									0.44
(7)	9-15	$\lambda\lambda = 4064$	<0.04										0.12
(11)	3-3	5380.2	1.55 ± 15%	1.6	0.76	1.15	1.20	2.75	1.10	1.25	0.55	0.71	2.24
(12)	3-5	5052.1	1.60 ± 12%	1.7		1.27	1.61	4.20		1.30		0.86	1.94
(13)	3-1	4932.0	3.58 ± 15%	4.6	2.20	3.4	4.63	8.6	3.5	3.5	1.3	1.5	5.22
(14)	3-3	4371.3	0.54 ± 25%	0.97		0.4							1.21
(16)	3-5	4269.0	0.21 ± 25%	0.32		0.23							0.41
(17)	3-1	4228.3	0.60 ± 40%										1.70
(18)	15-9	$\lambda\lambda = 5798$	0.30 ± 20%	0.39	0.21				0.24	0.30	0.21	0.17	
	7-5	5793.5	0.33	0.33									
	5-5	5794.5	0.33 ± 30%	0.06									
	3-5	5794.8	0.004	0.004									
	5-3	5801.1	0.32 ± 30%	0.29									
	3-3	5800.2	0.01	0.01									
	3-1	5805.8	0.13 ± 40%	0.39									
(22)	3-3	6587.8	1.3 ± 30%	2.4									2.21

^a Johansson (Ref. 28) classifies this multiplet as $2p^3 D_3 - 4f (3^1/2)_{3,4}$, in which case the A value obtained in this work would be $0.17 \times 10^6 \text{ sec}^{-1}$.

demixing, Henning² ran pure carbon plasmas in a Kiel-type arc, relying on ratios of C II to C I line intensities to deduce source temperatures.

Doherty³ measured the relative strengths of carbon and hydrogen lines in the emission from a luminous shock tube. Results of these ($A_C^{I,H}$) determinations are larger than present A values by factors of 1.2–2.8. Doherty also measured absolute strengths for several neutral neon lines, obtaining results generally a factor of 2 smaller than those¹¹ reported later. A plausible explanation for this pattern of disagreements, as suggested by Fig. 1, is a systematic overestimate (~10%) of experimental temperature in Doherty's work.

Singly ionized carbon

Conditions were suitable in only eight experiments (temperatures > 12 500 °K and exposure times > 30 μ sec) for recording the two most readily excited visible C II lines, $\lambda = 6578.0$ and $\lambda = 6582.9$. Under these conditions, however, lines normally used as internal A value standards [H_{β} , NeI ($\lambda = 5852 \text{ \AA}$)] were too bright and exceeded the dynamic range of our emulsions. With reliable transpecies relative A -value determinations precluded by emulsion saturation, and with determinations via the emission (i.e., A_{CII}^{em}) method ruled out by the critical dependence of emitter densities on source temperature, we measured the ratio $A(\lambda = 6578)/A(\lambda = 6583)$. Our result ($0.93 \pm 15\%$) agrees satisfactorily with the value (1.00) predicted by LS coupling.

Neutral sulfur

Stark broadening completely blended the fine structure of visible SI multiplets under all shock-tube conditions. The red multiplets ($\lambda\lambda = 6049 \text{ \AA}$) and ($\lambda\lambda = 5701 \text{ \AA}$) were detected with regularity, but these features were too diffuse (half-widths of more than 50 \AA) to be handled in a quantitative

way. The quality of SI profiles was generally poorer than CI and SII data recorded at the same time because of pronounced broadening and inherent weakness. Multiplets (1), (2), (3) could not be investigated for want of sufficiently fast infrared emulsions.

Neutral sulfur A values measured with the shock-tube and comparison data appear in Table IV. The A values reported by Bridges and Wiese⁶ were obtained by photoelectrically scanning a wall-stabilized arc. Foster^{4,5} used a vortex-stabilized arc as the source of SI (and CI) spectra. Tabulated integrals of radial transition moments³⁰ and LS coupling coefficients were used to calculate the A values listed in the last columns of the table.

The three sets of experimental relative SI strengths agree more closely with one another than with theoretical calculations. The shock-tube findings confirm one observed feature in the solar curve of growth^{32,33}: namely, that the calculated strength of the $4s^5S-5p^5P$ multiplet is too large by at least a factor of 2 relative to the strength of the $4p^5P-5d^5D$ multiplet.

Present results differ in absolute value from earlier data, being factors of 1.2–1.6 smaller, and factors of 1.1–1.2 larger, respectively, than the findings of Bridges and Wiese⁶ and of Foster.^{4,5} Our results are in agreement with the value measured by Schulz-Gulde.⁸

Compared to our data, Coulomb approximations for SI are too large by factors of 1.3–3.0, whereas our CI data agreed satisfactorily. Because of this disparity, and to check the internal consistency of the experiments, we measured the strength of SI ($\lambda\lambda = 4695 \text{ \AA}$) directly against the CI ($\lambda = 5052 \text{ \AA}$) A value. Gases such as CS_2 and CH_3SH assured fixed abundance ratios in the shock tube. These measurements ($A_S^{I,C}$ in the notation of Sec. II) involved only a mild susceptibility to errors in experimental temperature; and these optically thin lines do not differ markedly in brightness, shape, or wavelength. The A value

TABLE IV. Neutral sulfur transition probabilities.

Multiplet number	Multiplet	$g_i - g_k$	λ (\AA)	Transition probability (10^6 sec^{-1})					Coulomb approximation ³⁰
				This work	Bridges and Wiese ⁶	Foster ⁷	Schulz-Gulde ⁸	NBS ¹²	
2	$4s^5S^0 - 5p^5P$	5-15	4695	$0.66 \pm 20\%$	1.03	0.58	0.667	0.74	2.0
4	$4s^3S^0 - 5p^3P$	3-9	5279	$0.46 \pm 22\%$	0.54	0.35		0.38	0.88
5	$4s^3S^0 - 6p^3P$	3-9	4411	<0.05					Cancellation
7	$4p^5P - 6s^5S^0$	15-5	7690	$7.8 \pm 25\%$				6.1	6.1
8	$4p^5P - 5d^5D^0$	15-25	6751	$9.5 \pm 25\%$	11.0			7.9	7.5
10	$4p^5P - 6d^5D^0$	15-25	6049	<0.20					Cancellation
11	$4p^5P - 7d^5D^0$	15-25	5701	<0.08					Cancellation

of S I ($\lambda\lambda = 4695 \text{ \AA}$) found in this way, $0.64 \times 10^6 \text{ sec}^{-1}$, agrees closely with the value ($0.66 \times 10^6 \text{ sec}^{-1}$) obtained from $\frac{1}{2}(A_{S \text{ II}}^{\text{em}} + A_{S \text{ II}}^{\text{H}})$ data.

Ionized sulfur

The $A_{S \text{ II}}^{\text{r,H}}$ and the $A_{S \text{ II}}^{\text{r,Ne}}$ data, shown in Fig. 6 for S II ($\lambda = 5453 \text{ \AA}$) were generally obtained simultaneously. The $A_{S \text{ II}}^{\text{r,Ne}}$ determinations utilize a reference line [Ne I ($\lambda = 5852$)] which resembles S II ($\lambda = 5453 \text{ \AA}$) in excitation potential, wavelength, shape, and brightness better than does H_{β} . This is offset by the greater uncertainty in the Ne I ($\lambda = 5852 \text{ \AA}$) A value.¹² Treating the two determinations as being equally reliable yielded the S II ($\lambda = 5453 \text{ \AA}$) A -value data shown in Fig. 6. The value adopted is $1.0 \times 10^8 \text{ sec}^{-1}$.

Absolute S II transition probabilities from this investigation are compared with published values in Table V. In most instances, data reduction was not complicated by blending or optical depth problems.

Agreement between this work and the absolute and relative A values of Bridges and Wiese⁶ is excellent, the average absolute-value ratio $A_{\text{Bridges}}/A_{\text{This work}}$ being 0.97. This agreement is perplexing in contrast to the factor of (1.2-1.6) discrepancies between the absolute S I results from the same two experiments. Bias in either sulfur abundance or temperature cannot alone account for this pattern or for agreement and disagreement. The likelihood of coupled errors appears remote for the shock tube which is not subject to serious demixing and where the ratio $(A_{S \text{ I}}^{\text{em}} + A_{S \text{ I}}^{\text{r,H}})/(A_{S \text{ II}}^{\text{r,Ne}} + A_{S \text{ II}}^{\text{r,H}})$ is comparatively insensitive to uncertainties in temperature data.

Schulz-Gulde⁸ measured the transition prob-

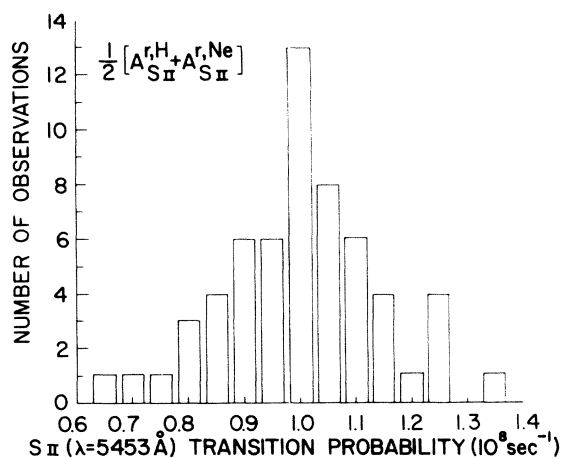


FIG. 6. Histogram of results from simultaneous measurement of the S II ($\lambda = 5453 \text{ \AA}$) absolute transition probability by two techniques.

ability of S II ($\lambda = 5453 \text{ \AA}$) to be $0.71 \times 10^8 \text{ sec}^{-1}$ using a wall-stabilized arc. This is in agreement within error estimates with present results.

Working with a vortex-stabilized arc,^{4, 5} Foster has found³³ a value of $0.78 \times 10^8 \text{ sec}^{-1}$ for absolute transition probability of S II ($\lambda = 5453 \text{ \AA}$). Allowing for joint experimental uncertainties, this result satisfactorily overlaps the findings of Bridges and Wiese⁶ and the present work.

Calculations in the Coulomb approximation tend to underestimate the shock-tube and wall-regulated-arc data by factors of 1.1-1.6.

We computed the sums from measured, array-averaged f values for transitions involving the 4s and 4p configurations with the one-electron Thomas-Reiche-Kuhn³⁴ sum rule ($\sum_{n'} f_n^{n'} = 1$) and the Wigner-Kirkwood³⁴ partial sum rules

$$\sum_{n'} f_{nl}^{n'l-1} = -\frac{1}{3} \frac{l(2l-1)}{2l+1};$$

$$\sum_{n'} f_{nl}^{n'l+1} = \frac{1}{3} \frac{(l+1)(2l+3)}{2l+1}.$$

In forming the sums, shock-tube data were augmented by hydrogenic approximations for high-quantum-number lines and bound-free transitions. For the 4s level the f values summed to 1.3, rather than the 1.0 expected from the one-electron model. This disagreement appears due primarily to the large measured strength of the 4s-4p transition array. The f values listed in Ref. 12 (Coulomb approximations) agree somewhat better, approaching 1.1. It is not clear what modifications should be made in the one-electron sum rules to account for transitions involving equivalent electrons, or that all pertinent levels have been properly classified.⁶ For these reasons it is not felt that the 30% discrepancy between our 4s data should necessarily be attributed to experimental error.

By adopting hydrogenic approximations for several unobserved arrays, we can compare measured f sums with the partial sum rules for the 4p level. Agreement with the sum rule is found within experimental and computational uncertainty.

Table VI compares relative S II line strengths. Data are normalized by assigning value 1.00 to the ($\lambda = 5453 \text{ \AA}$) transition probability. Agreement between the arc⁶ and shock-tube data is impressive: 92% of the relative strengths overlap within our experimental uncertainties [(4-14)%]. By the same criteria, 66% of the intermediate-coupling predictions³⁶ agree with our data. Only 17% of LS coupling calculations agree. Considering how the two sets of experimental data reinforce each other, this comparison is felt to provide a compelling argument for the desirability of

TABLE V. Transition probabilities for ionized Sulfur (10^6 sec^{-1}).

Multiplet ²⁹	Transition	$J_i - J_k$	λ (Å)	This work ^a	Bridges and Wiese ⁶	NBS ¹²	Coulomb approximation		
							L S Coupling	Intermediate coupling (Ref.35)	(Ref.36)
(1)	$3s3p^4 2P - 4p^2 S^0$	$1\frac{1}{2} - \frac{1}{2}$	5027.1	0.46C	$0.36 \pm 40\%$				
		$\frac{1}{2} - \frac{1}{2}$	5142.3	0.27A					
(2)	$3s3p^4 2P - 4p^4 P^0$	$1\frac{1}{2} - 1\frac{1}{2}$	4121.0	0.05E					
(6)	$4s^4 P - 4p^4 D^0$	$2\frac{1}{2} - 3\frac{1}{2}$	5453.6 ^b	1.01A	$1.00 \pm 35\%$	0.78	0.77	0.78	0.85
		$1\frac{1}{2} - 2\frac{1}{2}$	5432.7	0.77A	$0.78 \pm 35\%$	0.61	0.55	0.62	0.68
		$\frac{1}{2} - 1\frac{1}{2}$	5428.6	0.55A	$0.50 \pm 35\%$	0.38	0.33	0.38	0.42
		$2\frac{1}{2} - \frac{1}{2}$	5564.9	0.20A	$0.20 \pm 35\%$	0.16	0.22	0.16	0.17
		$1\frac{1}{2} - 1\frac{1}{2}$	5509.6	0.42A	$0.45 \pm 45\%$	0.39	0.40	0.37	0.40
		$\frac{1}{2} - \frac{1}{2}$	5473.6	0.84A	$0.86 \pm 35\%$	0.74	0.64	0.66	0.73
		$2\frac{1}{2} - 1\frac{1}{2}$	5645.6 ^c	0.19E ^c		0.018	0.04	0.02	0.02
		$1\frac{1}{2} - \frac{1}{2}$	5556.0	0.29B		0.15	0.12	0.10	0.11
(7)	$4s^4 P - 4p^4 P^0$	$2\frac{1}{2} - 2\frac{1}{2}$	5032.4	0.84B	$0.87 \pm 35\%$	0.66	0.68	0.76	0.81
		$1\frac{1}{2} - 1\frac{1}{2}$	4991.9	0.38C		0.15	0.13	0.08	0.33
		$\frac{1}{2} - \frac{1}{2}$	4942.4	0.35C		0.15	0.17	0.14	0.15
		$2\frac{1}{2} - 1\frac{1}{2}$	5103.3	0.34D		0.50	0.43	0.64	0.27
		$1\frac{1}{2} - \frac{1}{2}$	5009.5	1.07B		0.70	0.82	0.86	0.94
		$1\frac{1}{2} - 2\frac{1}{2}$	4924.1	0.40A		0.22	0.30	0.22	0.24
		$\frac{1}{2} - 1\frac{1}{2}$	4925.3			0.24	0.43	0.24	0.51
(8)	$4s^4 P - 4p^2 D^0$	$2\frac{1}{2} - 2\frac{1}{2}$	4779.1	0.06E		0.64			
(9)	$4s^4 P - 4p^4 S^0$	$2\frac{1}{2} - 1\frac{1}{2}$	4815.5	1.08D	$0.94 \pm 35\%$	0.64	0.55	0.34	0.88
		$1\frac{1}{2} - 1\frac{1}{2}$	4716.2	0.36C	$0.34 \pm 35\%$	0.23	0.39	0.50	0.29
		$\frac{1}{2} - \frac{1}{2}$	4656.7	0.19C		0.12	0.19	0.33	0.09
(11)	$3d^4 F - 4p^4 D^0$	$4\frac{1}{2} - 3\frac{1}{2}$	5606.1	0.38A	$0.40 \pm 35\%$	0.30	0.22		
		$3\frac{1}{2} - 2\frac{1}{2}$	5640.3 ^c	0.49E ^c			0.20		
		$2\frac{1}{2} - 1\frac{1}{2}$	5659.9	0.44A	$0.43 \pm 45\%$	0.34	0.19		
		$1\frac{1}{2} - \frac{1}{2}$	5664.7	0.52A	$0.48 \pm 35\%$	0.38	0.24		
		$3\frac{1}{2} - 3\frac{1}{2}$	5526.2	0.09C		0.081	0.026		
		$2\frac{1}{2} - 2\frac{1}{2}$	5578.8	0.11C		0.074	0.04		
		$1\frac{1}{2} - 1\frac{1}{2}$	5616.6	0.18E		0.083	0.05		
		$1\frac{1}{2} - 2\frac{1}{2}$	5536.7	0.10D		0.066	0.002		
(14)	$4s^2 P - 4p^2 D^0$	$1\frac{1}{2} - 1\frac{1}{2}$	5819.2	0.11D	$0.12 \pm 40\%$	0.085	0.114	0.12	0.09
		$\frac{1}{2} - 1\frac{1}{2}$	5646.9 ^c	0.49E ^c		0.68	0.57	0.67	0.57
		$1\frac{1}{2} - 2\frac{1}{2}$	5639.9 ^c	0.63E ^c		0.75	0.68	0.76	0.66
(15)	$4s^2 P - 4p^2 P^0$	$1\frac{1}{2} - 1\frac{1}{2}$	5014.0	0.98C		0.72	0.87	0.92	0.84
		$\frac{1}{2} - \frac{1}{2}$	4917.1	0.84D		0.55	0.70	0.73	0.66
		$\frac{1}{2} - 1\frac{1}{2}$	4885.6	0.14E		0.13	0.17	0.15	0.17
(29)	$3d^2 F - 4p^2 F^0$	$3\frac{1}{2} - 3\frac{1}{2}$	3993.5	0.08D					
		$3\frac{1}{2} - 2\frac{1}{2}$	4007.8	0.03D					
(32)	$3d^2 P - 4p^2 D^0$	$1\frac{1}{2} - 2\frac{1}{2}$	4431.0	0.09E					
(36)	$3d^2 D - 4p^2 D^0$	$2\frac{1}{2} - 2\frac{1}{2}$	4668.6	0.31E					
		$1\frac{1}{2} - 1\frac{1}{2}$	4648.2	0.29E					
(38)	$4s^2 D - 4d^2 F^0$	$2\frac{1}{2} - 3\frac{1}{2}$	5320.7	1.01A	$1.16 \pm 35\%$	0.84			0.91
		$1\frac{1}{2} - 2\frac{1}{2}$	5345.7	1.24C	$1.15 \pm 35\%$	0.75			0.84
		$2\frac{1}{2} - 2\frac{1}{2}$	5345.7			0.11			0.06
(39)	$4s^2 D - 4d^2 D^0$	$2\frac{1}{2} - 2\frac{1}{2}$	5212.6	1.86C		0.72			0.85
		$1\frac{1}{2} - 2\frac{1}{2}$	5212.6			0.098			0.02
		$1\frac{1}{2} - 1\frac{1}{2}$	5201.0	1.66C		0.68			0.75
		$2\frac{1}{2} - 1\frac{1}{2}$	5201.3			0.065			0.13
(40)	$4s^2 D - 4d^2 P^0$	$2\frac{1}{2} - 1\frac{1}{2}$	4524.9	0.97C		0.98			1.15
		$1\frac{1}{2} - 1\frac{1}{2}$	4524.7			0.093			0.27
(43)	$4p^4 D^0 - 5s^4 P$	$3\frac{1}{2} - 2\frac{1}{2}$	4463.6	0.76D		0.53	0.71		
		$2\frac{1}{2} - 1\frac{1}{2}$	4483.4	0.40E		0.31	0.44		
		$1\frac{1}{2} - \frac{1}{2}$	4486.7	0.86E		0.66	0.55		
		$1\frac{1}{2} - 1\frac{1}{2}$	4432.4	0.09E		0.29	0.24		
(44)	$4p^4 D^0 - 4d^4 F$	$3\frac{1}{2} - 4\frac{1}{2}$	4162.7	2.6D		2.3	2.18		
		$2\frac{1}{2} - 3\frac{1}{2}$	4153.1	1.2E		2.0	1.88		
		$1\frac{1}{2} - 2\frac{1}{2}$	4145.1	1.1D		1.8	1.65		
(45)	$4p^4 D^0 - 4d^4 D$	$3\frac{1}{2} - 3\frac{1}{2}$	4028.8	0.39D		0.51	0.47		

TABLE V. (Continued)

Multiplet ²⁹	Transition	$J_i - J_k$	λ (Å)	This work ^a	Bridges and Wiese ⁶	NBS ¹²	Coulomb approximation	
							LS Coupling	Intermediate coupling (Ref. 35) (Ref.36)
(46)	$4p\ ^4P^0 - 5s\ ^4P$	$2\frac{1}{2} - 2\frac{1}{2}$	3990.9	0.22 <i>D</i>		0.35	0.32	
		$3\frac{1}{2} - 2\frac{1}{2}$	4050.1	0.12 <i>D</i>		0.11	0.10	
		$2\frac{1}{2} - 1\frac{1}{2}$	4003.9	0.25 <i>D</i>		0.21	0.19	
		$2\frac{1}{2} - 2\frac{1}{2}$	4792.0	0.98 <i>D</i>		0.37	0.38	
		$2\frac{1}{2} - 3\frac{1}{2}$	4294.4 ^c	1.6 <i>D</i>		1.7	1.6	
		$1\frac{1}{2} - 2\frac{1}{2}$	4267.8	1.1 <i>D</i>		1.2	1.1	
		$\frac{1}{2} - 1\frac{1}{2}$	4269.8		0.70	0.65		
		$2\frac{1}{2} - 2\frac{1}{2}$	4318.7	0.65 <i>D</i>		0.49	0.45	
		$1\frac{1}{2} - 1\frac{1}{2}$	4282.6	0.93 <i>C</i>		0.89	0.82	
		$\frac{1}{2} - \frac{1}{2}$	4278.5	1.4 <i>D</i>		1.4	1.3	
(50)	$4p\ ^4P^0 - 4d\ ^4P$	$2\frac{1}{2} - 2\frac{1}{2}$	3892.3	1.2 <i>D</i>		0.63	0.56	
(55)	$4p\ ^2D^0 - 4d\ ^2F$	$1\frac{1}{2} - 2\frac{1}{2}$	3923.5	1.3 <i>D</i>		2.0	1.78	
(59)	$4p\ ^4S^0 - 4d\ ^4P$	$1\frac{1}{2} - 2\frac{1}{2}$	4032.8	0.4 <i>E</i>		1.2	1.10	
		$1\frac{1}{2} - 1\frac{1}{2}$	3998.1	0.7 <i>E</i>		1.2	1.09	
		$1\frac{1}{2} - \frac{1}{2}$	3979.9	0.8 <i>E</i>		1.2	1.11	
(66)	$4p\ ^2D^0 - 4d\ ^2F$	$2\frac{1}{2} - 3\frac{1}{2}$	4259.2	0.6 <i>E</i>		1.5		
		$1\frac{1}{2} - 2\frac{1}{2}$	4257.4		1.4			
		$2\frac{1}{2} - 2\frac{1}{2}$	4249.9	0.6 <i>E</i>		0.10		
(67)	$4p\ ^2D^0 - 4d\ ^2G$	$2\frac{1}{2} - 3\frac{1}{2}$	4231.0	1.7 <i>E</i>				

^a Estimated uncertainty: Absolute *A* values: 18% ≤ *A* < 22%, 22 ≤ *B* < 28%, 28% ≤ *C* < 38%, 38% ≤ *D* < 50%, *E* > 50%.

^b Foster (Ref. 33), using vortex-stabilized arc, determined the *A* value of $\lambda = 5453.6$ to be $0.78 \times 10^8 \text{ sec}^{-1}$. Schulz-Gulde (Ref. 8), using a wall-stabilized arc, found the *A* value of $\lambda = 5453.6$ to be $0.71 \times 10^8 \text{ sec}^{-1}$.

^c Line completely blended with a line of some other multiplet. Relative intensity lamp data have been used to unfold blends, so that results should be regarded as being uncertain by at least 50%.

using a coupling description sensitive to details of atomic level structure.

To see if configuration interactions have strong influence on line strengths in the $4s-4p$ transition array, we test for departures from *J*-file and *J*-group sum invariance.³⁷ In Table VII the ratios of measured file sums to file degeneracies are seen to vary by approximately 20%, with partic-

ularly large excursions occurring in the $4p\ ^4D^0_{1/2}$ and $4p\ ^2D^0_{3/2}$ columns. The uncertainty in our $3p4s-3p4p$ results is estimated to be slightly less than this discrepancy: misclassifications or configuration mixing be partially responsible. The *J*-group sums also scatter by ±20% from the *J*-group sum invariance associated with non-interacting arrays of the $\alpha s-\alpha p$ type.

TABLE VI. Comparison of relative SII *A* values.

Multiplet	λ (Å)	This work	Bridges ⁶ <i>et al</i>	LS ³⁷ coupling	IC ³⁵ coupling	IC ³⁶ coupling
(6)	5453.6	1.00 Ref	1.00	1.00	1.00	1.00
	5432.7	0.77 ± 0.03	0.78	0.71	0.79	0.79
	5428.6	0.55 ± 0.03	0.50	0.43	0.49	0.49
	5564.9	0.20 ± 0.02	0.20	0.28	0.21	0.20
	5509.6	0.42 ± 0.03	0.45	0.52	0.47	0.47
	5473.6	0.84 ± 0.03	0.86	0.83	0.85	0.86
(7)	5032.4	0.84 ± 0.04	0.87	0.88	0.97	0.95
(9)	4815.5	1.08 ± 0.15	0.94	0.71	0.44	1.03
	4716.2	0.36 ± 0.03	0.34	0.51	0.64	0.34
(11)	5606.1	0.38 ± 0.03	0.40	0.28
	5659.9	0.44 ± 0.03	0.43	0.25
	5664.7	0.52 ± 0.04	0.48	0.31
(14)	5819.2	0.11 ± 0.03	0.12	0.15	0.15	0.11
Fraction of transitions in agreement with present results			92%	17%	33%	67%

TABLE VII. *J*-file sum rule for ionized sulfur 4s-4*p* transition array.

Configuration $3p^2(^3P)4p$	$^2S_{1/2}^0$	$^2P_{1/2}^0$	$^4P_{1/2}^0$	$^4D_{1/2}^0$	$^4S_{3/2}^0$	$^2P_{3/2}^0$	$^4P_{3/2}^0$	$^2D_{3/2}^0$	$^4D_{3/2}^0$	$^4P_{5/2}^0$	$^2D_{5/2}^0$	$^4D_{5/2}^0$	$^4D_{7/2}^0$	File sum File weight
$^2P_{1/2}$	4.0 ^b	9.9	0 ^a	0 ^a	0 ^a	3.3	0 ^a	17.4	0 ^a					17.3
$^4P_{1/2}$	0 ^a	0 ^a	3.7	13.6	1.7	0 ^a	9.3	0.03 ^b	17.4					22.8
$^2P_{3/2}$	9.3 ^b	4.0 ^b	0 ^a	0 ^a	0 ^a	24.4	0 ^a	4.3	0 ^a	0 ^a	33.4	0 ^a		18.9
$^4P_{3/2}$	0 ^a	0 ^a	11.8	8.7	6.6	0 ^a	8.3	0.01 ^b	13.9	14.0	0.09 ^b	36.6		25.0
$^4P_{5/2}$					21.2	0 ^a	7.9	0.07 ^b	6.0	28.2	1.7	10.2	64.6	23.3
File sum File weight	6.7	7.0	7.8	11.1	7.4	6.9	6.4	5.5	9.3	7.0	8.8	7.8	8.1	

^a Line too faint for detection.^b Calculated using intermediate coupling (Ref. 36).

IV. SUMMARY OF RESULTS

Absolute transition probabilities of 124 visible and infrared lines of CI, SI, and SII were measured in a consistent way. These data which are more complete and more stringently tested than any carbon or sulfur set previously available, are compared with other experiments, with re-

fining intermediate coupling calculations and with various sum rules.

ACKNOWLEDGMENTS

The authors wish to thank Joseph Clawson, Timothy Brennan, and David Koopman for their advice and assistance in reducing the data.

*Research supported in part by National Aeronautics and Space Administration Grant No. NGR 21-002-007/9 and by the Welch Foundation. Computer time was provided through NASA Grant No. NsG-398 to the Computer Science Center of the University of Maryland.

†Present address: Physics Department, Harvard University, Cambridge, Mass. 02138.

¹M. U. Beth, thesis (Kiel, 1963) (unpublished); J. Richter, *Z. Phys.* **151**, 114 (1958); C. Kuck, thesis (Kiel, 1955) (unpublished); H. Maecker, *Z. Phys.* **135**, 13 (1953).

²H. Hemming, *Z. Astrophys.* **62**, 109 (1965).

³L. R. Doherty, thesis (University of Michigan, 1962) (unpublished).

⁴E. W. Foster, *Proc. Phys. Soc. Lond.* **79**, 94 (1962).

⁵E. W. Foster, *Proc. Phys. Soc. Lond.* **80**, 882 (1962).

⁶J. M. Bridges and W. L. Wiese, *Phys. Rev.* **159**, 31 (1967).

⁷E. W. Foster, *Proc. Phys. Soc. Lond. A* **90**, 275 (1967).

⁸E. Schulz-Gulde, *Z. Phys.* **245**, 308 (1971).

⁹W. D. Arnett and J. W. Turnan, *Astrophys. J.* **157**, 339 (1969); H. Reeves and E. E. Salpeter, *Phys. Rev.* **116**, 1505 (1959).

¹⁰D. L. Lambert and B. Warner, *Mon. Not. R. Astr. Soc.* **138**, 181 (1968); D. L. Lambert, *Mon. Not. R. Astr. Soc.* **138**, 143 (1968); L. Goldberg, E. A. Müller, and L. H. Aller, *Astrophys. J. Suppl.* **5**, 1 (1960); A. G. W. Cameron, *Astrophys. J.* **129**, 676 (1959).

¹¹W. L. Wiese, M. W. Smith, and B. M. Glennon, *U. S. Natl. Bur. Stds. Misc. Pub.* **278** (1966).

¹²W. L. Wiese, M. W. Smith, and B. M. Glennon, *Atomic Transition Probabilities*, Natl. Bur. Stds. Res. Ser. 4 (U. S. GPO, Washington, D. C., 1966), Vol. I; *ibid.*,

Vol. II (1970).

¹³J. Richter, in *Plasma Diagnostics*, edited by W. Lochte-Holtgreven (Wiley-Interscience, Amsterdam, 1968); D. Robinson and P. Lenn, *Appl. Opt.* **6**, 893 (1967); E. W. Foster, *Rep. Prog. Phys.* **27**, 469 (1964); J. Cooper, *Rep. Prog. Phys.* **29**, 35 (1966); H. R. Griem, *Plasma Spectroscopy* (McGraw-Hill, New York, 1964).

¹⁴D. H. Sampson, General Electric Tech. Inform. Ser. No. R64SD90, 1964 (unpublished); H. R. Griem, *Phys. Rev.* **131**, 1170 (1963); R. W. P. McWhirter, in *Plasma Diagnostic Techniques*, edited by R. H. Huddleston and S. L. Leonard (Academic, New York, 1965).

¹⁵A. T. Hattenburg, *Appl. Opt.* **6**, 195 (1967).

¹⁶M. H. Miller and R. D. Bengtson, *J. Quant. Spectr. Radiat. Transfer* **9**, 1573 (1969).

¹⁷H. R. Griem, *Phys. Rev.* **128**, 997 (1962); D. W. Koopman, University of Maryland Tech. Note BN-481, 1966 (unpublished); J. C. Rich and J. C. Flagg, Harvard College Observatory Sci. Rep. No. 12, 1966 (unpublished).

¹⁸M. H. Miller, *J. Quant. Spectrosc. Radiat. Transfer* **9**, 1251 (1969).

¹⁹S. M. Wood and M. H. Miller, *Rev. Sci. Instrum.* **41**, 1196 (1970).

²⁰M. H. Miller, R. A. Roig, and R. D. Bengtson, *Phys. Rev. A* **4**, 1709 (1971); R. D. Bengtson, M. H. Miller, D. W. Koopman, and T. D. Wilkerson, *Phys. Rev. A* **3**, 16 (1971); M. H. Miller and R. D. Bengtson, *Phys. Rev. A* **1**, 983 (1970).

²¹M. H. Miller, University of Maryland Tech. Note BN-550, 1968 (unpublished).

²²R. D. Bengtson, M. H. Miller, D. W. Koopman and

- T. D. Wilkerson, *Phys. Fluids* **13**, 372 (1970).
- ²³I. I. Glass and G. Hall, *Handbook of Supersonic Aerodynamics*, NAVORD Rep. No. 1488, 1959 (unpublished); Y. B. Zel'dovich and Y. P. Raizer, *Physics of Shock Waves and High-Temperature Hydrodynamic Phenomena*, (Academic, New York, 1968).
- ²⁴W. R. S. Garton, W. H. Parkinson and E. M. Reeves, *Proc. Phys. Soc. Lond.* **88**, 771 (1966).
- ²⁵R. H. Tourin, *Spectroscopic Gas Temperature Measurement* (Elsevier, Amsterdam, 1966).
- ²⁶P. Kepple and H. R. Griem, *Phys. Rev.* **173**, 317 (1968).
- ²⁷R. A. Bell, R. D. Bengtson, D. R. Branch, D. M. Gottlieb, and R. A. Roig, University of Maryland Tech. Note. BN-72 (unpublished).
- ^{27a}Note added in proof. Stuck and Wende [*Phys. Rev. A* **9**, 1 (1974)] measure the transition probability of C I ($\lambda = 5052 \text{ \AA}$) to be $(1.4 \pm 0.3) \times 10^6 \text{ sec}^{-1}$ in agreement with present results.
- ²⁸L. Johansson, *Ark. Fys.* **31**, 201 (1966).
- ²⁹C. E. Moore, *A Multiplet Table of Astrophysical Interest* (rev. ed.) Natl. Bur. Stds. Tech. Note No. 36 (1959).
- ³⁰G. Oertel and L. P. Shomo, *Astrophys. J. Suppl.* **145** (1969).
- ³¹D. R. Bates and A. Damgaard, *Astrophys. J.* **107**, 383 (1948).
- ³²D. L. Lambert and B. Warner, *Mon. Not. R. Astr. Soc. Lond.* **138**, 181 (1968); J. P. Swings, D. L. Lambert, and N. Grevese, *Solar Phys.* **6**, 3 (1969).
- ³³E. W. Foster, *J. Phys.* **33**, L146 (1970).
- ³⁴H. A. Bethe and E. E. Salpeter, *Quantum Mechanics of One- and Two-Electron Atoms* (Springer, Berlin, 1957).
- ³⁵R. H. Garstang, *Mon. Not. R. Astr. Soc.* **114**, 118 (1954).
- ³⁶M. Aymar, *Physica (Utrecht)* **66**, 364 (1973).
- ³⁷E. U. Condon and G. H. Shortly, *The Theory of Atomic Spectra* (Cambridge U. P., Cambridge, England, 1963).